Prediction and experimental measurement of the electromagnetic thrust generated by a microwave thruster system*

Yang Juan(杨 涓)†, Wang Yu-Quan(王与权), Ma Yan-Jie(马艳杰), Li Peng-Fei(李鹏飞), Yang Le(杨 乐), Wang Yang(王 阳), and He Guo-Qiang(何国强)

College of Astronautics, Northwestern Polytechnical University, Xi'an 710072, *China*

(Received 16 March 2012; revised manuscript received 29 December 2012)

A microwave thruster system that can convert microwave power directly to thrust without a gas propellant is developed. In the system, a cylindrical tapered resonance cavity and a magnetron microwave source are used respectively as the thruster cavity and the energy source to generate the electromagnetic wave. The wave is radiated into and then reflected from the cavity to form a pure standing wave with non-uniform electromagnetic pressure distribution. Consequently, a net electromagnetic thrust exerted on the axis of the thruster cavity appears, which is demonstrated through theoretical calculation based on the electromagnetic theory. The net electromagnetic thrust is also experimentally measured in the range from 70 mN to 720 mN when the microwave output power is from 80 W to 2500 W.

Keywords: electromagnetic waves, Maxwell stress tensor, electromagnetic processes and properties

PACS: 03.50.De, 41.20.Jb, 13.40.–f **DOI:** 10.1088/1674-1056/22/5/050301

1. Introduction

The conventional space plasma thrusters, such as Hall thrusters and ion thrusters, are space propulsion devices with high performance, high reliability, and long life duration. These thrusters can control and position satellites accurately and power deep space spacecrafts used for asteroid detection and moon sensing.[1–8] A solar sail is another space propulsion device that can move forward without consuming gas propellant as long as it can collect sufficient energy from sunlight.[9] This concept has been known for more than a century, but the feasibility of the solar sail technology has just been demonstrated by a Japanese space yacht, called IKAROS.[10] A microwave-propelled sail closely resembles a solar sail. A thin metal mesh forms a sail that is pushed by microwave radiation or Poynting flux from a separate ground microwave source.[11] Relying on a propellantless solar sail or a microwave-propelled sail instead of conventional electric propulsion provides the spacecraft with flexibility during flight.

We have designed and fabricated another new type of thruster: the microwave thruster. The key component of the thrust is a cylindrical tapered resonant cavity, which can also be pushed by microwave radiation, the same as sun photons hitting a huge solar sail at a right angle and the Poynting flux directing exactly to a huge metal mesh. The different between this system and the microwave sail is that the microwave source and the tapered resonant cavity are integrated together, while they are separated in the microwave sail. This property makes the microwave thruster compact, highly efficient, and easy to control the thrust level.

Shawyer has worked on this new type of propulsion for some time. He called the device the Emdrive. In September 2006, New Scientist reported[12] that Shawyer had constructed a prototype unit weighing 9 kg which consumes 700 W power and produces 88 mN force. In May 2007, Eureka magazine reported[13] that a second unit has been built for demonstration purposes, weighing 100 kg, consuming 300 W for microwave production, and producing 96.1 mN force.

In 2008, Northwestern Polytechnical University took interest in this new concept thruster, which is they called the propellantless microwave thruster. Nowadays, considering the only medium in the thruster system is microwave fields, they call it the microwave thruster. They have explained the theory behind this new propulsion according to the electromagnetic theory and developed their first experimental model based on the microwave resonant cavity theorem. With a developed force-feedback thrust stand, the developed model was experimentally demonstrated to generate a net electromagnetic (EM) thrust from 70 mN to 720 mN when the microwave output power was from 80 W to 2500 W. This article presents the work. The structure of the new concept thruster is given in Section 2. The explanation on the EM thrust exerted on the cylindrical tapered resonance cavity is presented in Section 3, together with the interpretation of the EM thrust induced by a traveling microwave. The total net EM thrust prediction is given in Section 4. The force-feedback stand and the measurement results of the total net EM thrust from the microwave thruster are showed in Section 5. The conclusion is given in Section 6.

*Project supported by the National Natural Science Foundation of China (Grant No. 90716019).

†Corresponding author. E-mail: yangjuan@nwpu.edu.cn

© 2013 Chinese Physical Society and IOP Publishing Ltd

2. Structure of the microwave thruster

As shown in Fig. 1, a microwave thruster can have two kinds of structure. In Fig. 1(a), the thruster comprises a microwave source, waveguides 1–3, a circulator, and a cylindrical tapered resonant cavity or thruster cavity, where the terminal of waveguide 3 is opened to atmosphere or outer space. The microwave source is used to generate a continuous microwave that is radiated into the thruster cavity through waveguide 1, the circulator, and waveguide 2, and then reflected from the cavity to atmosphere or outer space through waveguide 2, the circulator, and waveguide 3. In this process, like light acting on a solar sail, the radiating microwave also generates an EM pressure on every wall surface of the microwave parts (waveguide, circulator, and thruster cavity), where the integral of the EM pressure along the wall surfaces will form the EM thrust. As shown in Fig. 1(a), inside the waveguides and the circulator, the microwave field normally has an axially symmetrical distribution, therefore the EM pressure acting on one side surface is equal to that on the opposite side, i.e., $p_4 = p_5$, $p_6 = p_7$, $p_8 = p_9$, $p_{10} = p_{11}$, $p_{12} = p_{13}$, and the associated EM force has the same relation, i.e., $F_5 = F_6$, $F_7 = F_8$, $F_9 = F_{10}$, $F_{11} = F_{12}$, $F_{13} = F_{14}$, which leads to zero total EM force perpendicular to the side wall surfaces of the waveguides and the circulator. The only non-zero EM force, shown as F_{15}, F_{16}, F_{17}, F_{18}, and F_{19} in Fig. 1(a), is along the axial direction. However the axial EM force is too weak to be observed due to the wave in traveling or non resonant state. The thruster cavity is a key component that is developed based on the theory of microwave resonant cavity. If the cavity is elaborately designed and attains a resonant mode, then the phase of the incident wave at any point inside of the thruster cavity will be equal to the reflected one, and the amplitude of the total wave will be a direct summation of the two waves, which leads to a pure standing EM wave and an obvious EM pressure. If the microwave resonant mode inside the thruster cavity is carefully chosen, on the inner wall of the thruster cavity, a special EM pressure distribution can be formed to produce a net axial EM thrust which is large enough to be observed. Therefore it can be arranged so that the EM thrust mainly comes from the thruster cavity.

In the structure shown in Fig. 1(a), the open waveguide 3 will lead to serious microwave leakage, which interferes with the environment. As shown in Fig. 1(b), this problem can be properly resolved by using a matched load to absorb the reflected microwave beam. The matched load attached to the open waveguide 3 will change the reflected microwave into radiated heat in the atmosphere or outer space through its radiator. Thus this thruster system can avoid the microwave leakage; meanwhile the additional EM thrust generated by the matched load is also too weak to be considered for the traveling wave state. Due to the exchange between microwave or heat and atmosphere or outer space, both the thruster systems are opened, and the system shown in Fig. 1(b) is appropriate for actual use.

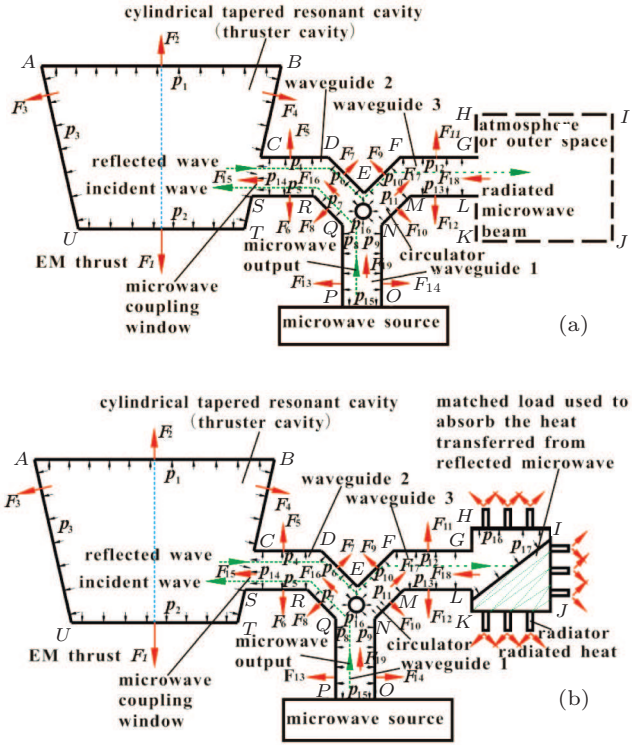


Fig. 1. (color online) Microwave thruster systems with (a) reflected microwave radiating to atmosphere or outer space and (b) reflected microwave energy being transferred to heat which is radiated to atmosphere or outer space through a matched load.

3. Theory of EM thrust exerted on the boundary of a limited closed volume filled by a microwave

3.1. EM thrust exerted on the boundary of a limited closed volume filled by a traveling microwave

When an EM wave travels in free space, an EM thrust will appear on the boundary of a chosen limited closed volume V according to the Maxwell equation and the Poynting flux vector or energy flux density vector. In the process of thrust generation, the EM wave acts as the medium which will exchange momentum and energy between the limited closed volume and its outside space. Meanwhile the total momentum and the total energy of the medium are conserved. The following deduction will verify the statement.

Resorting to charged particles floating in an EM field can make the statement deduction easily understandable and acceptable. The charged particles will be exerted by the electric force of microwave, $\rho \boldsymbol{E}$, which is the Coulomb force, where ρ is the charge quantity in a unit volume, and $\boldsymbol{E}$ is the electric field of the microwave. The electric force instantly will force the charged particles to move and generate an oriented current in the unit volume, therefore the charged particles again are exerted by the magnetic force of microwave, $\boldsymbol{J} \times \boldsymbol{B}$, which is

the Lorentz force, where $\boldsymbol{B}$ is the magnetic field of the microwave, and $\boldsymbol{J}$ is the current density of the moving particles. According to Newton's second law, the momentum $\boldsymbol{g}_{\rm p}$ of the charged particles in the unit obeys

$$\frac{\partial \boldsymbol{g}_{\rm p}}{\partial t} = \rho \boldsymbol{E} + \boldsymbol{J} \times \boldsymbol{B}. \tag{1}$$

Obviously only the electric field works on the charged particles because the Lorentz force is always perpendicular to the particle velocity. According to the law of conservation of energy, the energy $w_{\rm p}$ of the charged particles in the unit obeys

$$\frac{\partial w_{\rm p}}{\partial t} = \boldsymbol{J} \cdot \boldsymbol{E}. \tag{2}$$

From the Maxwell equations, it can be deduced that

$$\frac{\partial}{\partial t}(w_{\rm p}+w_{\rm f})+\nabla \cdot \boldsymbol{S} = 0, \tag{3}$$

where $\boldsymbol{S} = \boldsymbol{E} \times \boldsymbol{H}$ and $w_{\rm f}= \boldsymbol{E} \cdot \boldsymbol{D}/2 + \boldsymbol{H} \cdot \boldsymbol{B}/2$ respectively present the energy flux density vector and the energy density of the EM wave. In terms of the Gauss divergence law and within the limited closed volume, Eq. (3) can be integral as

$$\oint_S \boldsymbol{S} \cdot \boldsymbol{n} \mathrm{d}S = -\frac{\partial}{\partial t} \int_V (w_{\rm p}+w_{\rm f}) \mathrm{d}V = 0. \tag{4}$$

By differentiating vector $\boldsymbol{S}$ with respect to time, considering the Maxwell equation, and applying the differential parallel vector equation, then

$$\begin{aligned} &\frac{\partial}{\partial t}(\mu_0 \varepsilon_0 \boldsymbol{S} + \boldsymbol{g}_{\rm p}) \\ &= -\boldsymbol{\nabla} \cdot \left[\left(\frac{1}{2}\varepsilon_0 E^2 + \frac{1}{2}\mu_0 H^2 \right) \boldsymbol{I} - \varepsilon_0 \boldsymbol{E}\boldsymbol{E} - \mu_0 \boldsymbol{H}\boldsymbol{H} \right]. \end{aligned} \tag{5}$$

Set $\boldsymbol{g}_{\rm f}= \mu_0 \varepsilon_0 \boldsymbol{S}$, obviously $\boldsymbol{g}_{\rm f}$ is the momentum density of the EM field. By considering Maxwell tensor $\boldsymbol{T} = -\frac{1}{2}(\varepsilon_0 E^2 + \mu_0 H^2)\boldsymbol{I} + \varepsilon_0 \boldsymbol{E}\boldsymbol{E} + \mu_0 \boldsymbol{H}\boldsymbol{H}$, in terms of the Gauss divergence law and within the limited closed volume, Eq. (5) can be integral as

$$\frac{\partial}{\partial t} \int_V (\boldsymbol{g}_{\rm f}+\boldsymbol{g}_{\rm p}) \mathrm{d}V = \oint_S \boldsymbol{n} \cdot \boldsymbol{T} \mathrm{d}S. \tag{6}$$

Then for the only EM field where $\boldsymbol{g}_{\rm p} = 0$ and $w_{\rm f} = 0$, equations (4) and (6) will be

$$\frac{\partial}{\partial t} \int_V (w_{\rm p}) \mathrm{d}V = 0, \tag{7}$$

$$\frac{\partial}{\partial t} \int_V (\boldsymbol{g}_{\rm f}) \mathrm{d}V = \oint_S \boldsymbol{n} \cdot \boldsymbol{T} \mathrm{d}S. \tag{8}$$

Equations (7) and (8) demonstrate that the energy and the momentum of the EM field within the limited closed volume are separately conserved and correspond to Newton's second law. Obviously the right hand of Eq. (8) is the EM force exerted on the EM field boundary of the limited closed volume. According to Newton's third law, the boundary of the limited closed volume also will be acted by the force $-\oint_S \boldsymbol{n} \cdot \boldsymbol{T} \mathrm{d}S$.

3.2. EM thrust exerted on the boundary of thruster cavity filled by a pure standing microwave

As Fig. 2 shown, at any point of the thruster cavity inner wall, a Descartes reference frame (x,y,z) and its unit vector directions $(\boldsymbol{i}_x, \boldsymbol{i}_y, \boldsymbol{i}_z)$ are defined, then the electric components of the Maxwell tensor are

$$\begin{aligned} \boldsymbol{T}_{\rm e} &= \varepsilon_0 E \boldsymbol{i}_x E \boldsymbol{i}_x - \frac{1}{2}\varepsilon_0 E^2 (\boldsymbol{i}_x \boldsymbol{i}_x + \boldsymbol{i}_y \boldsymbol{i}_y + \boldsymbol{i}_z \boldsymbol{i}_z) \\ &= \frac{1}{2}\varepsilon_0 E^2 (\boldsymbol{i}_x \boldsymbol{i}_x - \boldsymbol{i}_y \boldsymbol{i}_y - \boldsymbol{i}_z \boldsymbol{i}_z). \end{aligned} \tag{9}$$

When taking the external normal direction of the cavity surface as positive, the electric component of the EM pressure is $\boldsymbol{P}_{\rm e}= -\boldsymbol{T}_{\rm e} \cdot \boldsymbol{n} = -\frac{1}{2}\varepsilon_0 E^2 \boldsymbol{i}_x$.

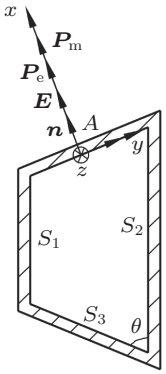


Fig. 2. Thruster cavity.

By neglecting the effect of microwave coupling window on the EM field and assuming the field is axial symmetrical, the total electric thrust exerted on the axis of the thruster cavity is $F_{\rm e}= \iint_{S_1} \frac{1}{2}\varepsilon_0 E^2 \mathrm{d}S - \iint_{S_2} \frac{1}{2}\varepsilon_0 E^2 \mathrm{d}S + \int_{S_3} \frac{1}{2}\varepsilon_0 E^2 \cos\theta \mathrm{d}S$, where S_1 and S_2 are the minor and the major end plate surfaces, respectively, and S_3 is the side wall surface. For a time harmonic EM wave, the electric intensity varies with time as trigonometric sines, which can be explained by electric plurality $\boldsymbol{E}(r,t) = \mathrm{Re}\left[\dot{\boldsymbol{E}}(r)\, \mathrm{e}^{\mathrm{j}\omega t}\right]$, where Re represents the real part. Therefore the total average electric thrust within a wave cycle and acted on the axis of the cavity is[14]

$$\begin{aligned} \langle F_{\rm e} \rangle &= \int_0^T F_{\rm e} \mathrm{d}t/T \\ &= \iint_{S_1} \frac{1}{4}\varepsilon_0 \mathrm{Re}\left(\dot{\boldsymbol{E}} \cdot \dot{\boldsymbol{E}}^*\right) \mathrm{d}S - \iint_{S_2} \frac{1}{4}\varepsilon_0 \mathrm{Re}\left(\dot{\boldsymbol{E}} \cdot \dot{\boldsymbol{E}}^*\right) \mathrm{d}S \\ &\quad + \iint_{S_3} \frac{1}{4}\varepsilon_0 \mathrm{Re}\left(\dot{\boldsymbol{E}} \cdot \dot{\boldsymbol{E}}^*\right) \cos\theta \mathrm{d}S, \end{aligned} \tag{10}$$

where $\dot{\boldsymbol{E}}^*$ is the conjugate complex of $\dot{\boldsymbol{E}}$. With the same method, the total average magnetic thrust within a wave cycle is given by

$$\langle F_{\rm m} \rangle = \int_0^T F_{\rm m} \mathrm{d}t/T$$

$$= \iint_{S_1} \frac{1}{4}\mu_0 \mathrm{Re}\left(\dot{\boldsymbol{H}} \cdot \dot{\boldsymbol{H}}^*\right) \mathrm{d}S - \iint_{S_2} \frac{1}{4}\mu_0 \mathrm{Re}\left(\dot{\boldsymbol{H}} \cdot \dot{\boldsymbol{H}}^*\right) \mathrm{d}S + \iint_{S_3} \frac{1}{4}\mu_0 \mathrm{Re}\left(\dot{\boldsymbol{H}} \cdot \dot{\boldsymbol{H}}^*\right) \cos\theta \, \mathrm{d}S. \quad (11)$$

When the EM wave is transmitted into the thruster cavity from the coupling window, the wave will be completely reflected back after encountering the metallic wall. As a result, the incident and the reflective EM waves at any point are in equi-phase. The two waves then superpose and form a resonant or pure standing EM wave with an augmented amplitude that is far larger than that of the incident wave, which leads to the augmentation of electric and magnetic power. According to the microwaves theory,[15] when a cavity is in the resonant state, a very low EM wave power level is damped by the cavity to maintain the wall skin effect. Therefore even the power stored in the electric and magnetic field is augmented, the total power absorbed by the resonant cavity is still only used to maintain the wall skin effect, which means that the total power stored in the resonant cavity is in the conservation state. This can be explained by using a parallel *RLC* loop operating on low frequency.

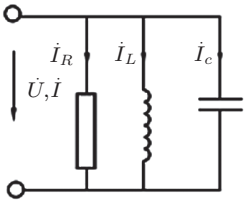


Fig. 3. Parallel *RLC* loop.

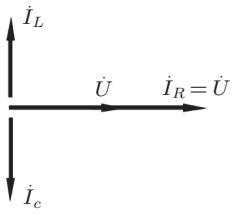


Fig. 4. The current and voltage of the resonant *RLC* loop.

As shown in Figs. 3 and 4, when a parallel *RLC* loop is in the resonant state, the capacitive reactance is completely the same as the inductive reactance. Correspondingly, currents going through the capacitance and the inductance are equal but the directions are opposite; the total power stored in the capacitance and the inductance is zero. It can be deduced that when the power in the capacitance is in a real form, P_a, the power in the inductance must be in an equivalent unused imaginary form, $-P_a$, hence the total power in the parallel *RLC* loop will be consumed only by the resistance. The structure of the *RLC* loop can be properly designed to have a very large quality factor, i.e., Q_{RLC}=$P_a/\left|\dot{I}_R\dot{U}\right| \gg 1$, and make P_a much larger than the total power $\left|\dot{I}_R\dot{U}\right|$. Therefore even the energy in the capacitance and the inductance is augmented by the *RLC* loop, the total energy in the *RLC* loop is still a constant, which does not violate the energy conservation law.

A hollow microwave resonant cavity is evolved from the *RLC* loop.[15] In the cavity, the power damped by the wall skin effect, P_r, stored in electric and magnetic fields, P_e, P_h, correspond to the power consumed by the resistance and stored in the capacitance and the inductance of the *RLC* loop, respectively. Therefore the parameters of the cavity also have $|P_e| = |P_h| = Q_{cavity}P_r = Q_{cavity}P_{input}$, where Q_{cavity} and P_{input} are the cavity quality factor and the power consumed by the microwave resonant cavity, respectively. As the above ratiocination, P_e and P_h are the powers used to generate the EM force, hence the electric, magnetic, and total net EM thrusts are

$$\langle F_e \rangle = Q \iint_{S_1} \frac{1}{4}\varepsilon_0 \mathrm{Re}\left(\dot{\boldsymbol{E}} \cdot \dot{\boldsymbol{E}}^*\right) \mathrm{d}S - \iint_{S_2} \frac{1}{4}\varepsilon_0 \mathrm{Re}\left(\dot{\boldsymbol{E}} \cdot \dot{\boldsymbol{E}}^*\right) \mathrm{d}S + Q \iint_{S_3} \frac{1}{4}\varepsilon_0 \mathrm{Re}\left(\dot{\boldsymbol{E}} \cdot \dot{\boldsymbol{E}}^*\right) \cos\theta \, \mathrm{d}S, \quad (12)$$

$$\langle F_m \rangle = Q \iint_{S_1} \frac{1}{4}\mu_0 \mathrm{Re}\left(\dot{\boldsymbol{H}} \cdot \dot{\boldsymbol{H}}^*\right) \mathrm{d}S - \iint_{S_2} \frac{1}{4}\mu_0 \mathrm{Re}\left(\dot{\boldsymbol{H}} \cdot \dot{\boldsymbol{H}}^*\right) \mathrm{d}S + Q \iint_{S_3} \frac{1}{4}\mu_0 \mathrm{Re}\left(\dot{\boldsymbol{H}} \cdot \dot{\boldsymbol{H}}^*\right) \cos\theta \, \mathrm{d}S, \quad (13)$$

$$\langle F_t \rangle = \langle F_e \rangle + \langle F_m \rangle . \quad (14)$$

4. Prediction of EM thrust from microwave thruster

In Ref. [16], we applied the finite element method to numerically simulate the EM fields inside different cylindrical tapered resonant cavities resonating on the equivalent principal modes of TE_{011}, TE_{012}, TE_{111}, and TM_{011}, and calculated the relevant quality factors. Then the EM thrusts produced by the microwave thrusters with these different tapered resonant cavities were theoretically predicted. It was found that the thruster cavity made by copper and resonating on the equivalent TE_{011} mode has a quality factor 320400 and generates total net EM thrust 411 mN for 1000 W 2.45 GHz incident microwave.

Based on the numerical simulation of EM fields in Ref. [16] and with Eqs. (12)–(14), the electric, magnetic, and total net EM thrusts from the thruster cavity operating at different microwave power are calculated, as shown in Figs. 5–8. The thrust curves demonstrate that on the surfaces of the major and the minor end plates, the magnetic thrust is two orders of magnitude higher than the electric thrust; on the surface of the side wall, the magnetic thrust is three times of the electric thrust; the total net EM thrust directs to the minor end plate, and the total net EM thrust ranges from 20 mN to 259 mN when the incident microwave power is from 20 W to 200 W.

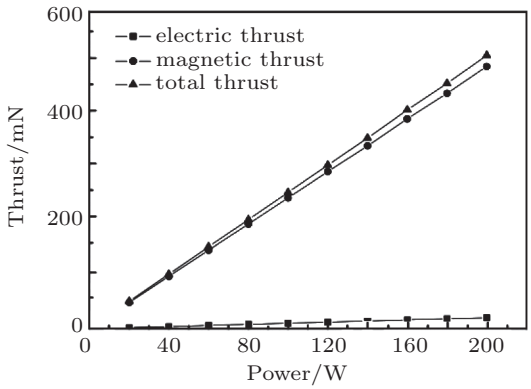


Fig. 5. Calculated thrusts on the major end plate and along its normal direction.

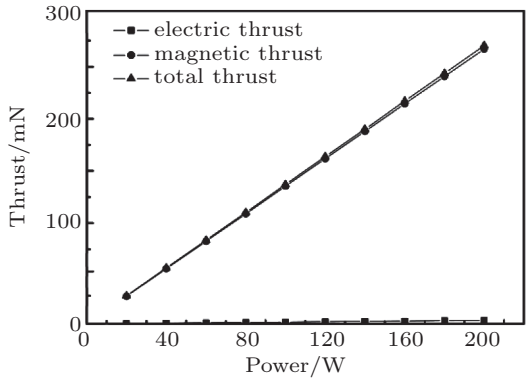


Fig. 6. Calculated thrusts on the minor end plate and along its normal direction.

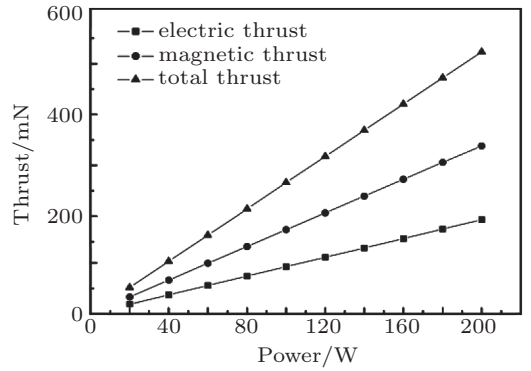


Fig. 7. Calculated thrusts on the side wall and along its normal direction.

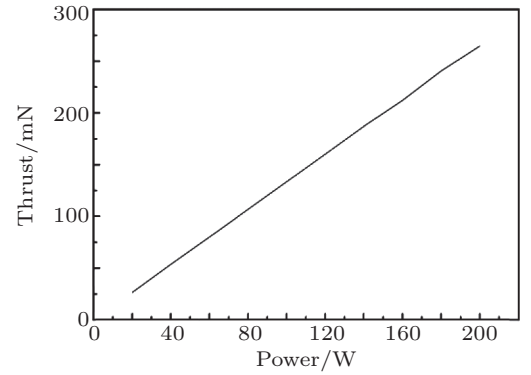


Fig. 8. Total net EM thrust along the normal direction of the minor end plate.

5. Thrust measurement system and experiment

5.1. Force-feedback thrust stand

As shown in Fig. 9, a force-feedback thrust stand is developed to conduct the EM thrust experiment. Combined with a part of the thruster system, the thrust stand depicted in Fig. 9 includes movable and immovable subsystems, and an electric circuit. The movable subsystem includes rigidly connected parts, such as thruster cavity (1), horizontal beam (2), the movable parts of left and right EM loops (3) and (4), swing plate (5), the movable parts of the angular displacement and acceleration transducers (6), support beams (7), counter weight (8), corrugated waveguide (9), and standard poise (10). The immovable subsystem includes rigidly connected parts, such as the immovable part of left and right EM loops (3) and (4), the immovable parts of the angular displacement and acceleration transducers (11), and the immovable subsystem poles (12). The electric circuit includes current amplifiers of the angular displacement and acceleration transducers, K_θ and $K_{\dot\theta}$, composite amplifier K_Σ, sampling resistance R, and a voltmeter. In the thruster stand, the line L_2 is decided by two pivots, on which the whole movable subsystem can swing within a small angle. As for the azimuth of the thruster cavity in Fig. 9, when the thruster operates, if the total net EM thrust directs to the minor end plate, the left EM loop (3) will be triggered to work. If the total net EM thrust is in the opposite direction, the right EM loop (4) will work.

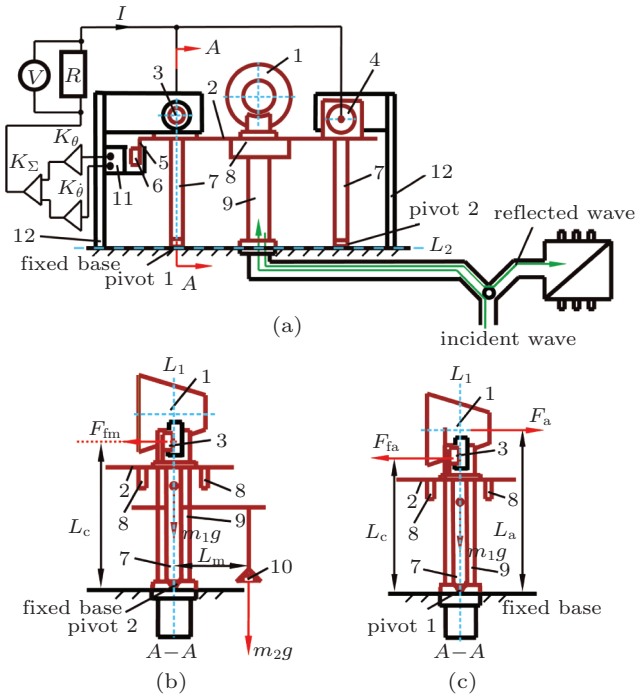


Fig. 9. (color online) Force-feedback thrust stand combined with a part of the microwave thruster system: (a) front view; (b) cut-away view when the stand is acted by the gravity force of a standard poise m_2g, and then balanced by the feedback force $F_{\rm fm}$ from the left EM loop; (c) cut-away view when the stand is acted by the EM thrust $F_{\rm a}$, and then balanced by the feedback force $F_{\rm fa}$ from the left EM loop.

The principle of the force-feedback thrust stand is that when a moment of EM thrust is exerted on the movable subsystem, it will swing around L_2 with a very small angle, and the movable parts of the angular displacement and acceleration transducers (6) will instantly trigger a feedback current I to the EM loop, subsequently a feedback force $F_{\rm fa}$ from the EM loop will produce a moment to balance that of the EM thrust, that is $F_{\rm a}L_{\rm a}=F_{\rm fa}L_{\rm c}$, where $F_{\rm a}$ is the EM thrust, $L_{\rm a}$ and $L_{\rm c}$ are the arms of the EM thrust and the EM loop feedback force, respectively. As a result, the movable subsystem is forced back to its original position. The moment generated by the EM loop can be known from the electric circuit parameters, hence the EM thrust can be deduced. In the thrust measuring, a key problem is the compensation of the elastic force from the corrugated waveguide and deleting the weight influence of the movable subsystem on the measured thrust.

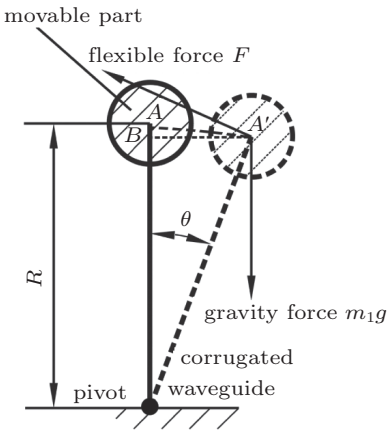


Fig. 10. Illustration of the balance between the moments acting on the movable subsystem.

To solve the key problem, the moment generated by the gravity force of the movable subsystem must be regulated to be equal to that from the waveguide elastic force. At this circumstance, as shown in Fig. 10, as soon as the movable subsystem swings a small angle due to the moment of the gravity force, the corrugated waveguide will generate another moment of elastic force. To balance the movable subsystem, we must have

$$FR = m_1 g L_{A'B}, \tag{15}$$

where F and R are the elastic force of the corrugated waveguide and its arm, respectively, m_1 and $L_{A'B}$ are respectively the mass of the movable subsystem and the arm of its gravity force. As $F = kL_{AA'}$, where k is the elastic coefficient of the corrugated waveguide, then $kL_{AA'}R = m_1 g L_{A'B}$, i.e., $k\theta RR = m_1 gR\sin\theta$. At the assumption of small angle θ, then $\sin\theta \approx \theta$, and from relation (15), we can deduce

$$kR = m_1 g. \tag{16}$$

Therefore, the parameters of the force-feedback thrust stand must be regulated and subjected to relation (16), then the elastic and the gravity forces will not affect the EM thrust measuring.

Another problem in thrust measurement is how to calculate the feedback force from the EM loop according to the structure of the thrust stand and the parameters of the electric circuit. This problem can be solved through calibration by standard poise. When the movable subsystem is only acted by the gravity force of the standard poise, the movable parts of the angular displacement and acceleration transducers also instantly trigger a feedback current I and induce a feedback force $F_{\rm fm}$ from the EM loop to balance the moment induced by the gravity force of the standard poise. Setting $L_{\rm a}=2L_{\rm m}$, where $L_{\rm m}$ is the arm of the standard poise gravity force, designing the electric circuit linearly, and properly choosing the voltmeter and the sampling resistance, then the voltmeter readout will be half of the standard poise gravity force. Actual calibration curves are portrayed in Fig. 11, which shows that the thrust stand has the linear property and the calibrated thrust is half of the standard poise gravity force. Due to the relation between $L_{\rm m}$ and $L_{\rm a}$, the effect of a half part of the standard poise gravity force, $m_2 g/2$, acted on the movable subsystem will be equivalent to that of the EM thrust. Therefore after calibrating, the measured EM thrust produced by the thruster cavity can be shown directly on the voltmeter of the sampling resistance.

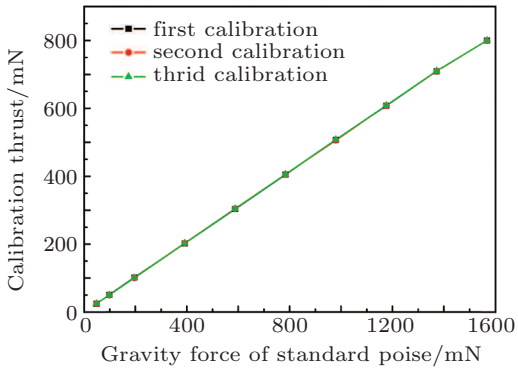


Fig. 11. (color online) Calibration curve of the thrust stand.

The third problem is to correct the float reading from the thrust measurement. Before the thrust stand is exerted by an additional force, it should be balanced to make the moments in the equilibrium state as shown in Eq. (15). At this circumstance, the readout of the measured thrust will be zero. After an additional force is exerted on the stand, the movable subsystem will swing with a very small angle, instantly the force will be balanced by the feedback force of the EM loop. At this case, the movable subsystem will return to its original state and the meter readout will give the measured value of the additional force. However after the additional force is removed, the corrugated waveguide will produce a very low additional elastic force and lead to a very low reading on the voltmeter,

the low reading is called float reading and must be subtracted from the measured value of the additional force.

5.2. Thrust measuring experiment and results

In the EM thrust measuring experiment, a magnetron is used as a microwave source to export continuous microwave power from 80 W to 2500 W at the frequency of 2.45 GHz, and the load can consume 2500 W microwave power.

To evaluate the thrust measuring precision, calibration error η_c, system error η_s, repeatability error η_r, and total error η_t are defined as

$$\eta_c = |m_2 g/2 - (F_{cal} - \varepsilon_0)| / (m_2 g/2) \times 100\%, \quad (17)$$

$$\eta_s = \sum_{i=1}^{n_{m1}} |\varepsilon_i| / \sum_{i=1}^{n_{m1}} |F_{i,cal} - \varepsilon_i| / n_{m1}, \quad (18)$$

$$\eta_r = \max\left(F_1 - \sum_{i=1}^{n_{m2}} F_i/n_{m2}, F_2 - \sum_{i=1}^{n_{m2}} F_i/n_{m2}, \ldots, F_{n_{m2}} - \sum_{i=1}^{n_{m2}} F_i/n_{m2},\right) / \sum_{i=1}^{n_{m2}} (F_i/n), \quad (19)$$

$$\eta_t = \max(\eta_c) + \eta_s + \eta_r, \quad (20)$$

where m_2 is the mass of the standard poise, F_{cal} and ε_0 are respectively the calibrated thrust and the float reading when the movable subsystem is acted by the standard poise, n_{m1} is the calibration sequence, ε_i and $F_{i,cal}$ are respectively the float reading and the thrust readout at the i-th time of calibration, n_{m2} is the EM thrust measuring sequence, and F_i denotes the measured EM thruster at the i-th time of experiment.

The experiment is first completed at the microwave output power ranging from 300 W to 2500 W. The result shows that the total net EM thrust direction is to the minor end plate. As shown in Fig. 12(a), the measured thrust varies nonlinearly with the microwave output power. The first maximum thrust is around 310 mN at 300 W microwave output power, and then the thrust will decrease to 160 mN when the power increases to 800 W. After that, the thrust will augment to 750 mN as the power increases to 2500 W. The second experiment is completed at the microwave output power ranging from 80 W to 1200 W, the results also show that the total net EM thrust direction is to the minor end plate. As shown in Fig. 12(b), the first maximum thrust is around 270 mN at 300 W microwave output power, and then the thrust will decrease to 180 mN when the power increases to 600 W. After that, the thrust will augment to 250 mN as the power increases to 1200 W. The experiments at the two power ranges demonstrate that the repeatability of thrust measuring is satisfying and the net EM thrust direction corresponds to the above theoretical calculation. However the measured relation between thrust and power is very different form the above calculation, which can be explained through the properties of the thruster cavity and the magnetron frequency spectrum.

According to the return loss testing method of the passive parts of microwave apparatus,[17] the resonating property of the thruster cavity can be tested with a microwave network analyzer. Figure 13 shows the measured relation between the frequency and the return loss of the thruster cavity. The return loss is defined as $L_r = 10\lg(P_r/P_i)$ (dB), where P_r and P_i are respectively the reflected and the incident microwave power. When L_r=0, the power is completely reflected from the cavity. At the point $L_r = L_{rmin}$, the power is reflected on a minimum level, which denotes that the cavity is in resonant state and the frequency is defined as resonant frequency f_0. We define the resonant frequency band as $\Delta f = f_2 - f_1$ at $L_r = 0.707 L_{rmin}$. Figure 13 shows that the resonant frequency and band are $f_0 = 2.450$ GHz and $\Delta f = 0.0016$ GHz, respectively. The circumstance shows that when the microwave output frequency ranges from 2.4492 GHz to 2.4508 GHz, more than 50% of microwave power can be absorbed by the resonant cavity to generate the EM thrust.

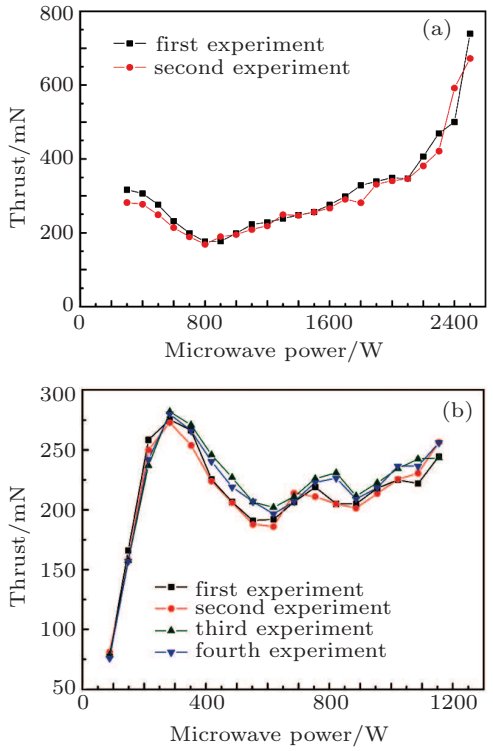


Fig. 12. (color online) Measured total net EM thrusts at microwave output power ranges (a) 300–2500 W and (b) 80–1200 W.

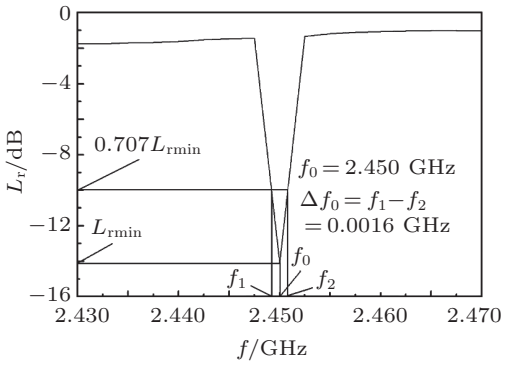


Fig. 13. The resonating property of thruster cavity in practical use.

The frequency spectrum of the magnetron used in the experiment can be measured using a spectral analyzer, as shown in Fig. 14. The curves demonstrate that within the thruster cavity frequency band, from 2.4492 GHz to 2.4508 GHz, the practical maximum microwave output power is 13 W, 120 W, 85 W, 65 W, 45 W, and 48 W respectively at the nominal output power 200 W, 300 W, 400 W, 500 W, 600 W, and 700 W. Therefore in Fig. 12(b), the measured thrusts 170 mN, 270 mN, 225 mN, 200 mN, 180 mN, and 210 mN at the nominal power 200 W, 300 W, 400 W, 500 W, 600 W, and 700W can be estimated to be generated by the practical microwave power 13 W, 120 W, 85 W, 65 W, 45 W, and 48 W, respectively. This relation shows that the EM thrust monotonously increases with the practical power augmentation, which presents almost the same trend as the above calculation.

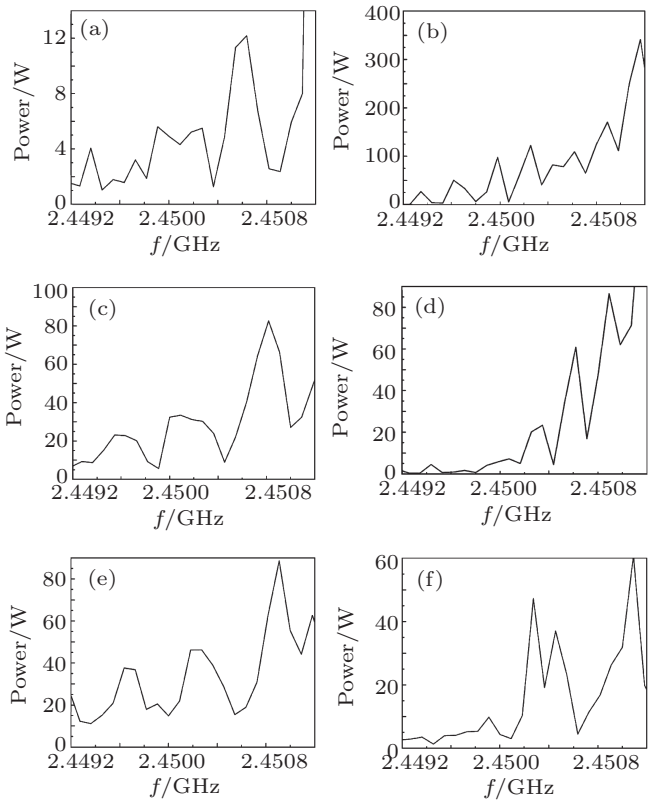


Fig. 14. Measured frequency spectra of the magnetron at the nominal power (a) 200 W, (b) 300 W, (c) 400 W, (d) 500 W, (e) 600 W, (f) 700 W.

Figure 15 gives the experiment errors. The measurements show that the total error is less than 12%. The highest repeatability error is 8%, which demonstrates that the precision of the thrust measuring system is acceptable and the microwave thruster system can definitely produce a net thrust.

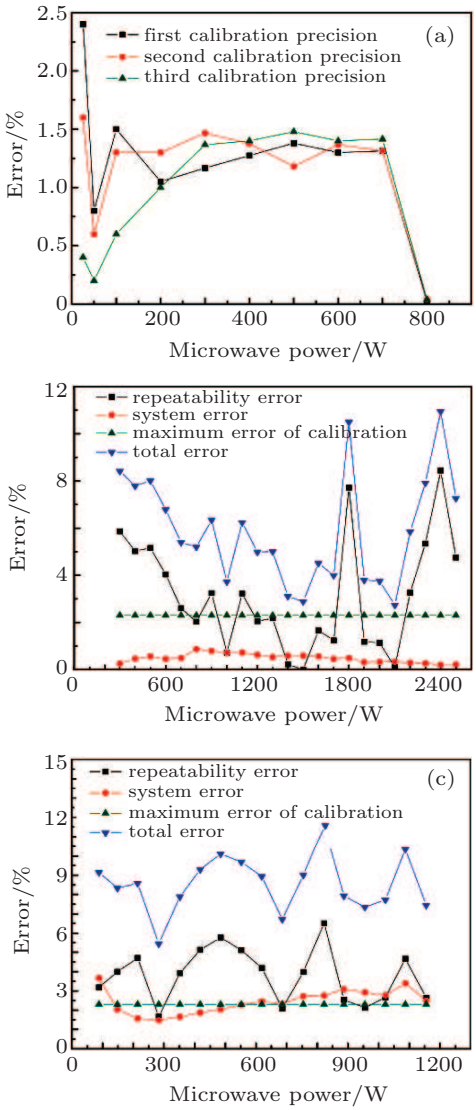


Fig. 15. (color online) Measured errors: (a) calibration error, (b) error at microwave output power of 300–2500 W, and (c) error at microwave output power of 80–1200 W.

6. Conclusion

The force-feedback thrust stand definitely demonstrates that the developed microwave thruster can generate a net EM thrust.

The thrust measurement experiment shows that the measured net EM thrust from the developed microwave thruster directs to the minor end plate of the thruster cavity. When the magnet output power ranges from 80 W to 2500 W, the thruster system will generate a net EM thrust from 80 mN to 720 mN. The thrust with the highest level is around 700 mN at the power of 2500 W. Meanwhile the thrust at a high level is around 270 mN at the power of 300 W. In other ranges, the EM thrust increases concomitantly with the increasing practical microwave output power. The thrust direction and the variation trend agree with the theoretical calculation.

References

[1] Kuninaka H, Nishiyama K, Funaki I, Yamada T, Shimizu Y and Kawaguchi J 2007 *Propuls. Power* **23** 544

[2] Kuninaka H, Nishiyama K, Funaki I, Shimizu Y, Yamada T and Kawaguchi J 2006 *Plasma Sci. IEEE Trans.* **34** 2125

[3] Funaki I, Kuninaka H, Toki K and Propuls J 2004 *Power* **20** 718

[4] Senguptaa A 2009 *Phys.* **105** 093303

[5] Smirnov A, Raitses Y and Fisch N J 2007 *Phys. Plasma.* **14** 057106

[6] Yang J, Han X W, He H Q and Mao G W 2004 *J. Spacecraft Rockets* **41** 126

[7] Yang J, Xu Y Q, Meng Z Q and Yang T L 2008 *Rev. Sci. Instrum.* **79** 083503

[8] Yang J, Xu Y Q, Tang J L, Mao G W, Yang T L and Tan X Q 2008 *Phys. Plasma* **15** 023503

[9] Johnson L, Young R M and Montgomery E E IV 2007 *AIP Conf. Proc.* **886** 207

[10] http://www.jaxa.jp/projects/sat/ikaros/index_e.html

[11] Abdallah C T, Chahine E, Geogriev D and Schamiloglu E 2003 *AIP Conf. Proc.* **664** 348

[12] Mullins J 2006 *New Sci.* **2568** 20

[13] Shelley T 2007 *Ureka*. **27** 14

[14] Wang Y P 2007 *Engineering Electrodynamics* (Xi'an: Xidian University Press) (in Chinese)

[15] Meng Q B 2005 *Microwave Technology* (Hefei: Industrial Press) (in Chinese)

[16] Yang J, Yang L, Zhu Y and Ma N 2010 *J. Northwestern Polytechnical University* **28** 807

[17] Yang J, He H Q, Mao G W and Han X W 2004 *J. Spacecraft Rockets* **41** 126

[18] Li K, Chen W J and Nao 2003 *Chin. Phys.* **12** 321

[19] Liu S T, Shi P F and Duan Y P 2010 *Acta Phys. Sin.* **59** 8566 (in Chinese)

[20] Liang C H and Tan K B 2009 *Acta Phys. Sin.* **58** 6770 (in Chinese)

[21] Nie N M, Huang J F and Zhao W J 2009 *Chin. Phys. B* **18** 2634

[22] Huang J Y and Li Y L 2005 *Chin. Phys. B* **14** 646